Peptide Helices as Rigid Molecular Rulers: A Conformational Study of Isotactic Homopeptides from α-Methyl-α-isopropylglycine, [L-(αMe)Val]$_n$**

Alessandra Polese, Fernando Formaggio, Marco Crisma, Giovanni Valle, Claudio Toniolo,* Gian Maria Bonora, Quirinus B. Broxterman, and Johan Kamphuis

Abstract: Terminally blocked, isotactic homopeptides from the sterically demanding α-methylvaline of general formula Y-[L-(αMe)Val]$_n$-O*t*Bu (Y = Z, *p*BrBz, Ac; $n = 2-8$) have been prepared step-by-step in solution and fully characterized. The conformations preferred in solution (β-turn and right-handed 3_{10}-helix) have been assessed by FT-IR, ^{1}H NMR and CD spectroscopy. The molecular and crystal structures of the Z-protected trimer, hexamer, heptamer and octamer have been determined by X-ray diffraction. In the crystal state, while the trimer is folded in a type III β-turn conformation, the longest homopeptides form well-developed, regular, right-handed 3_{10}-helices. The screw sense in the helix of the *p*BrBz-blocked octamer has been confirmed to be right-handed by solid-state and solution CD spectroscopy. The possible exploitation of these peptide helices as rigid and precise molecular rulers is discussed.

Keywords
amino acids · conformation · helices · molecular rulers · oligopeptides · structure elucidation

Introduction

Homooligopeptide helices of variable length have been widely exploited as end-to-end molecular rulers (also termed spacers, linkers or bridges) in spectroscopic studies. In this approach, distance dependencies of energy[1] and electron transfer,[1c, 2] and properties of biological macromolecular complexes[3] have been examined. In order to get reliable and correctly interpretable results, there is a need for stringently rigid molecular rulers. However, particularly in the case of the relatively short peptides that have been employed so far, only a restricted mobility has been achieved. In this context the most commonly used homopeptide series are (L-Pro)$_n$, followed by (Gly)$_n$, (L-Ala)$_n$, and γ-substituted (L-Glu)$_n$. Extensive investigations on (L-Pro)$_n$ oligomers have clearly shown the onset of different populations of multiple conformers arising from *cis*⇌*trans* (ω torsion angle) and *cis'*⇌*trans'* (ψ torsion angle) equilibria.[4] On the other hand, (Gly)$_n$ oligomers are known to fold in the ternary helix conformation, poly(Gly)$_n$I, or in the extended antiparallel β-sheet conformation, poly(Gly)$_n$II,[5] while (L-Ala)$_n$ and γ-substituted (L-Glu)$_n$ oligomers may adopt the α-helical or the β-sheet conformation.[5a, 6] In addition, in the complex conformational equilibria of short oligopeptides from C^α-trisubstituted (protein) amino acids, statistically disordered forms largely occur, their total population being inversely proportional to the peptide main-chain length.

As it is clear that none of the peptide series discussed above can produce truly rigid molecular rulers, in the last few years we have concentrated our efforts on homooligomeric series from the structurally restricted C^α-tetrasubstituted α-amino acids. In solution, pleionomers[7a] of the *achiral* Aib (α-aminoisobutyric acid or α,α-dimethylglycine), the prototype of this family of amino acids, form exclusively fully developed 3_{10}-helices[8] at the octamer level.[7] The helix percentage is still remarkably high (70–95%) for the oligomers from tetramer to heptamer. In the crystal state, however, all terminally blocked Aib oligomers form either type III (III') β-turns,[9] the basic structural unit of the 3_{10}-helix, or regular 3_{10}-helices.[7]

As part of our search for a homooligopeptide series based on an *optically active* C^α-tetrasubstituted glycyl residue, which inter alia would allow one to use chirospectroscopic techniques in structural analysis, we report herein the results of a detailed solid-state and solution conformational analysis of the terminally blocked, isotactic homopeptide series from α-methylvaline of general formula Y-[L-(αMe)Val]$_n$-O*t*Bu [Y = Z (benzyloxycarbonyl), *p*BrBz (*para*-bromobenzoyl), Ac (acetyl); $n = 2-8$; O*t*Bu, *tert*-butoxy]. This β-branched residue is even more sterically demanding than Aib itself. Among the various chiral amino acids of this family we selected (αMe)Val, as scattered conformational studies on very short homooligomers (dimer and trimer) and peptides clearly demonstrated that the relationship between the configuration of the (αMe)Val C^α atom and the screw sense of the structure formed is unequivocal and normal, that is, the all-L peptides give right-handed turns and helices, as found for protein amino acids.[10, 11]

[*] Prof. C. Toniolo, Dr. A. Polese, Dr. F. Formaggio, Dr. M. Crisma, Dr. G. Valle
Biopolymer Research Centre, CNR, Department of Organic Chemistry
University of Padova, 35131 Padova (Italy)
Fax: Int. code +(49)827-5239
Prof. G. M. Bonora
Pharmaco-, Chemico-, Technological Department
University of Cagliari, 09124 Cagliari (Italy)
Fax: Int. code +(70)658-521
Dr. Q. B. Broxterman, Dr. J. Kamphuis
DSM Research, Bioorganic Chemistry Section
P. O. Box 18, 6160 MD Geleen (The Netherlands)
Fax: Int. code +(46)767-604

[**] Linear Oligopeptides, Part 360. Part 359: A. Bianco, M. Maggini, G. Scorrano, C. Toniolo, G. Marconi, C. Villani, M. Prato, *J. Am. Chem. Soc.* **1996**, *118*, 4072–4080.

0947-6539/96/0209-1104 $ 15.00+.25/0

Results and Discussion

Synthesis and Characterization: For the large-scale production of the optically pure L-(αMe)Val we exploited an economically attractive, chemoenzymatic synthesis recently described by some of us.[12] We prepared a series of homopeptides of general formula Z-[L-(αMe)Val]$_n$-O*t*Bu from the dimer through to the octamer ($n = 2-8$). In the difficult coupling steps between two sterically demanding (αMe)Val residues the acid fluoride method[13a] afforded higher yields than the EDC/HOBt [EDC: 1-(3-dimethylaminopropyl)-3-ethylcarbodiimide, HOBt: 1-hydroxybenzotriazole],[13b] EDC/HOAt (HOAt: 1-hydroxy-7-azabenzotriazole)[13c] or the symmetrical anhydride method. The optimal conditions were found to be a modest excess (1.5 equiv) of the acid fluoride and 0.75 equiv of base (*N*-methylmorpholine). From selected Z-protected oligomers we also synthesized their Ac- and *p*BrBz-blocked analogues by treatment of the N-deprotected compounds with acetic anhydride in methylene chloride and with *para*-bromobenzoic acid/EDC/HOAt, respectively. Removal of the benzyloxycarbonyl N-protecting group was achieved by catalytic hydrogenation. Z-L-(αMe)Val-OH monohydrate, Z-L-(αMe)Val-O*t*Bu and [Z-L-(αMe)Val]$_2$O are known products.[10d] Z-L-(αMe)Val-F was prepared from the N-protected amino acid and cyanuric fluoride in pyridine.

The various peptides and their synthetic intermediates were characterized by melting point determination, optical rotatory power, thin-layer chromatography in three solvent systems, and solid-state IR absorption (Table 1).

Solid-state Conformational Analysis: We determined by X-ray diffraction the molecular and crystal structures of the four terminally blocked, isotactic homopeptides of general formula Z-[L-(αMe)Val]$_n$-O*t*Bu with $n = 3, 6-8$. The molecular structures with the atomic numbering schemes are illustrated in Figures 1–4. Relevant backbone and side-chain torsion angles are given in Table 2. In Table 3 the intra- and intermolecular H-bond parameters are listed.

All L-(αMe)Val residues, with the single exception of the slightly distorted C-terminal residue of the octamer, are found in the right-handed helical region of the conformational map. The average ϕ,ψ values of the residues completely involved in the helical structures are $-57, -29°$,[14] quite close to those expected for a right-handed 3_{10}-helix ($-57, -30°$).[8] The trimer forms a regular type III β-turn (Fig. 1). The single 1←4

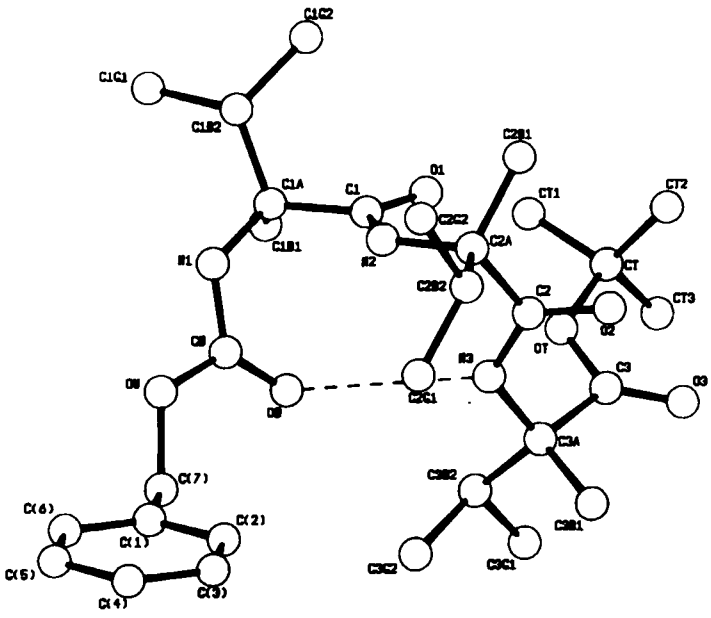

Fig. 1. Crystal structure of Z-[L-(αMe)Val]$_3$-O*t*Bu. The intramolecular H-bond is indicated by a dashed line.

C=O···H–N intramolecular H-bond has the N3···Oø distance at the upper limit of the expected range (2.8–3.2 Å).[15] Both molecules **A** and **B** in the asymmetric unit of the hexamer are folded in a right-handed 3_{10}-helical structure characterized by three 1←4 C=O···H–N intramolecular H-bonds in molecule **A**, and four in molecule **B** (Fig. 2). In the former the N5···O2 intramolecular distance, 3.525(5) Å, is too long for an H-bond. The heptamer (Fig. 3) and octamer (Fig. 4) also adopt well-developed, right-handed 3_{10}-helical structures, stabilized by five and six intramolecular H-bonds, respectively. The usual inversion of the handedness of the C-terminal helical residue with respect to that of the preceding ones[16] is not found in these 3_{10}-helix-forming peptide esters.

All urethane, peptide and ester groups are *trans*-planar (ω torsion angles), as expected, with only the urethane ω_0 torsion angle of molecule **B** and the peptide ω_3 angle of molecule **A** in the hexamer, and ω_6 of the octamer deviating more than 10° from planarity.[17] The major conformational difference between molecules **A** and **B** of the hexamer is seen in the $\chi^{1,1}$ and

Table 1. Physical properties and analytical data for the [L-(αMe)Val]$_n$ homopeptides.

Compound	M.p./°C [a]	Recryst. solvent [b]	$[\alpha]_D^{20}$ [c]	TLC [f] R_f(I)	R_f(II)	R_f(III)	IR $\tilde{\nu}$/cm^{-1} [h]
Z-L-(αMe)Val-F	oil	AcOEt–PE	2.7 [d]	0.85 [g]	–	–	3411,3339, 1836, 1698
Z-[L-(αMe)Val]$_2$-O*t*Bu	88–90	DE–PE	15.4	0.95	0.70	0.95	3408, 3389, 3304, 1718, 1657
Z-[L-(αMe)Val]$_3$-O*t*Bu	106–107	AcOEt–PE	9.6	0.95	0.95	0.95	3443, 3345, 1724, 1702, 1648
Z-[L-(αMe)Val]$_4$-O*t*Bu	199–201	AcOEt	7.2	0.95	0.50	0.95	3433, 3326, 1703, 1676
Z-[L-(αMe)Val]$_5$-O*t*Bu	190–191	AcOEt	14.4	0.90	0.45	0.95	3410, 3319, 1728, 1702, 1668
Z-[L-(αMe)Val]$_6$-O*t*Bu	185–186	AcOEt–PE	16.0	0.90	0.45	0.95	3424, 3334, 1704, 1662
Z-[L-(αMe)Val]$_7$-O*t*Bu	225–226	AcOEt–PE	15.1 [e]	0.85	0.45	0.95	3430, 3332, 1700, 1656
Z-[L-(αMe)Val]$_8$-O*t*Bu	230–232	$CHCl_3$–PE	20.3 [e]	0.85	0.40	0.95	3327, 1721, 1700, 1657
Ac-[L-(αMe)Val]$_4$-O*t*Bu	177–178	AcOEt–PE	8.2	0.80	0.40	0.95	3442, 3351, 3330, 1702, 1674
Ac-[L-(αMe)Val]$_6$-O*t*Bu	245–247	AcOEt–PE	16.3	0.75	0.40	0.95	3323, 1721, 1658
Ac-[L-(αMe)Val]$_8$-O*t*Bu	323–325	CH_2Cl_2–DE	11.4 [e]	0.70	0.30	0.95	3319, 1715, 1654
*p*BrBz-[L-(αMe)Val]$_8$-O*t*Bu	316–318	$CHCl_3$–DE	32.1 [e]	0.85	0.40	0.95	3325, 1719, 1656

[a] Determined on a Leitz model Laborlux 12 apparatus (Wetzlar, Germany). [b] AcOEt, ethyl acetate; PE, petroleum ether; DE, diethyl ether. [c] Determined on a Perkin-Elmer model 241 polarimeter (Norwalk, CT) equipped with a Haake model L thermostat (Karlsruhe, Germany): $c = 0.5$ (MeOH). [d] $c = 0.5$ (CH_2Cl_2). [e] $c = 0.5$ ($CHCl_3$). [f] Silica gel plates (60 F-254, Merck), solvent systems: (I) chloroform–ethanol 9:1; (II) toluene–ethanol 7:1; (III) butan-1-ol–acetic acid–water 6:2:2; the plates were developed with a UV lamp or with the hypochlorite–starch–iodide chromatic reaction, and a single spot was observed in each case. [g] Ethyl acetate–petroleum ether 3:1. [h] Determined in KBr pellets on a Perkin-Elmer model 580 B spectrophotometer equipped with a Perkin-Elmer model 3600 IR data station and a model 660 printer.

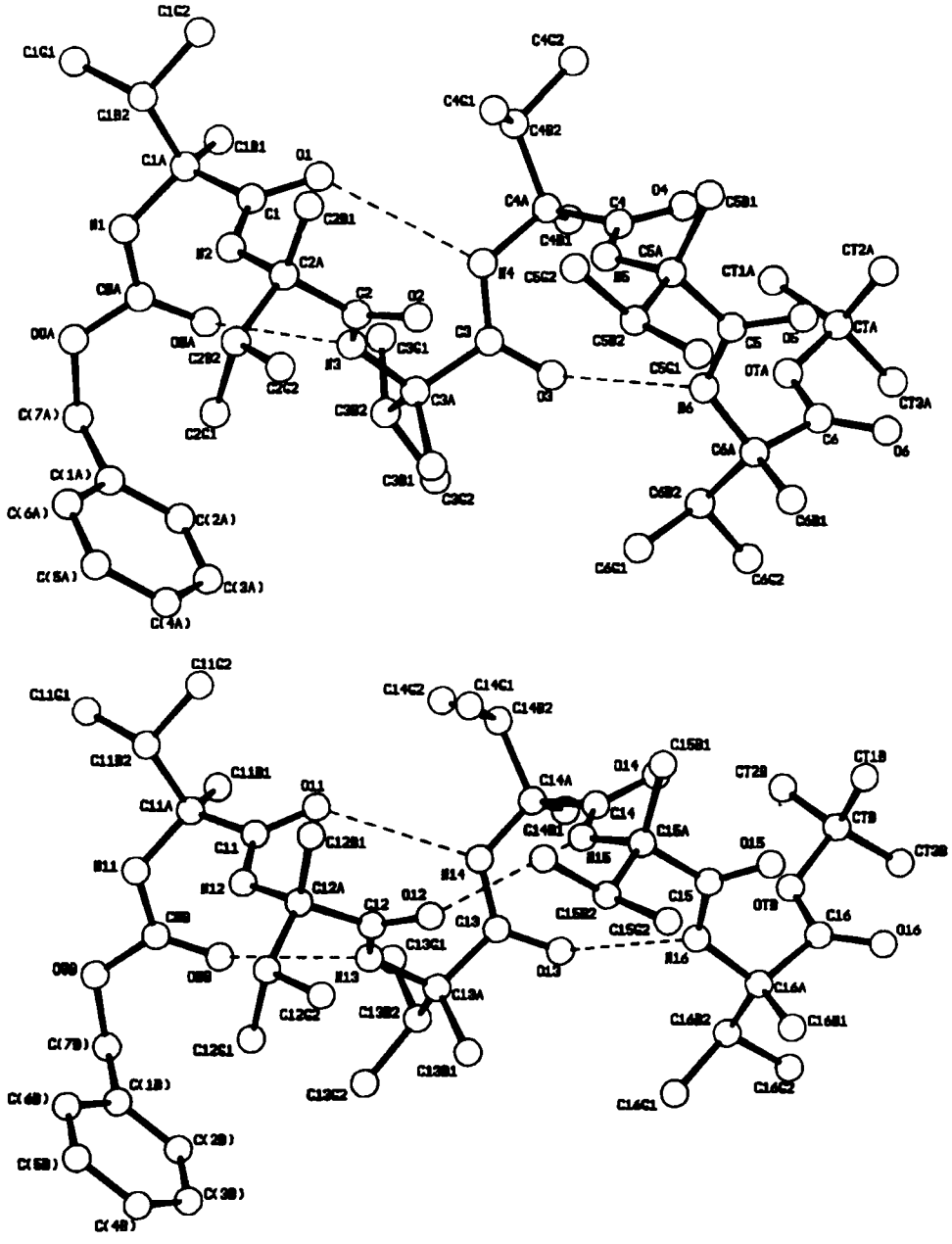

Fig. 2. Crystal structure of the two independent molecules A (top) and B (bottom) in the asymmetric unit of Z-[L-(αMe)Val]$_6$-O*t*Bu. The intramolecular H-bonds are indicated by dashed lines.

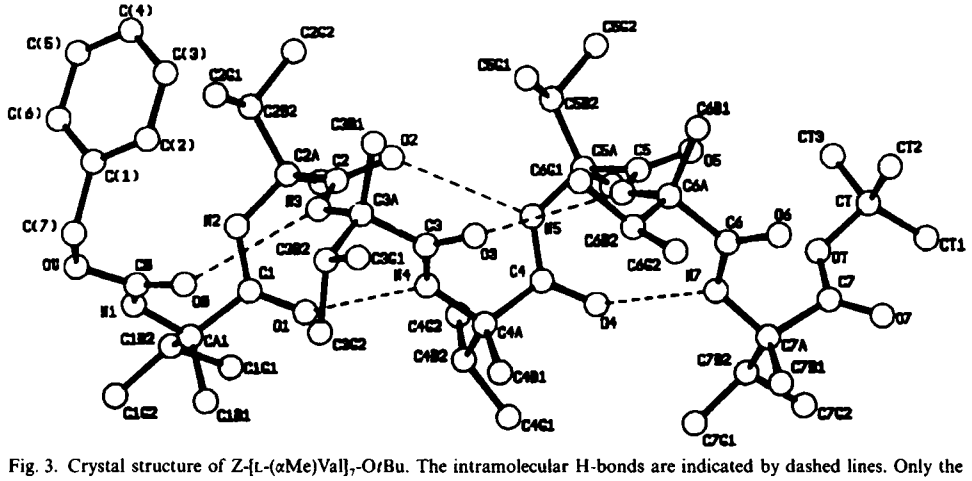

Fig. 3. Crystal structure of Z-[L-(αMe)Val]$_7$-O*t*Bu. The intramolecular H-bonds are indicated by dashed lines. Only the conformation with the higher occupancy factor for the C2G1 and C2G2 atoms is shown.

$\chi^{1,1'}$ side-chain torsion angles of residues 3 and 4 (g^+, t for the two residues of molecule **A**; g^+, g^- for the two residues of molecule **B**).[18]

In the packing mode of all the (αMe)Val oligomers, we find rows of molecules linked together either by urethane···peptide intermolecular H-bonds [N1–H···O2=C2 (in the trimer), N11–H···O5=C5 (between molecules **B** and **A** of the hexamer) and N1–H···O7=C7 (in the octamer)] or by urethane···ester intermolecular H-bonds [N1–H···O16=C16 (between molecules **A** and **B** of the hexamer) and N1–H···O7=C7 (in the heptamer)]. As usual, the N···O distances observed for intermolecular H-bonds are shorter than those typical of intramolecular H-bonds.

The screw sense of the helical structure that is formed by the octamer was confirmed by solid-state CD. The *para*-bromobenzamido chromophore at the N-terminus of a helical peptide chain was recently shown to be useful as a solid-state and solution CD probe in the determination of the relationship between the configuration of the C^α atom of the constituent amino acids and the peptide helix screw sense.[19] Figure 5B shows that the CD spectrum of *p*BrBz-[L-(αMe)Val]$_8$O*t*Bu is dominated by the contribution of the *para*-bromobenzamido chromophore, the absorption maximum of which is centred at 238–240 nm. A characteristically split CD curve is observed, with a positive Cotton effect at higher wavelengths, a negative Cotton effect at lower wavelengths and a cross-over point at 240 nm. This CD pattern is indicative of a right-handed peptide helical conformation.

Solution Conformational Analysis: The conformational preferences of the Z-[L-(αMe)Val]$_n$-O*t*Bu ($n = 2$–8) homopeptide series and the N^α–Ac and N^α–*p*BrBz octapeptides were investigated in $CDCl_3$, DMSO (dimethyl sulfoxide), TFE (2,2,2-trifluoroethanol) and HFIP (1,1,1,3,3,3-hexafluoro-

0947-6539/96/0209-1106 $ 15.00+.25/0 Chem. Eur. J. 1996, 2, No. 9

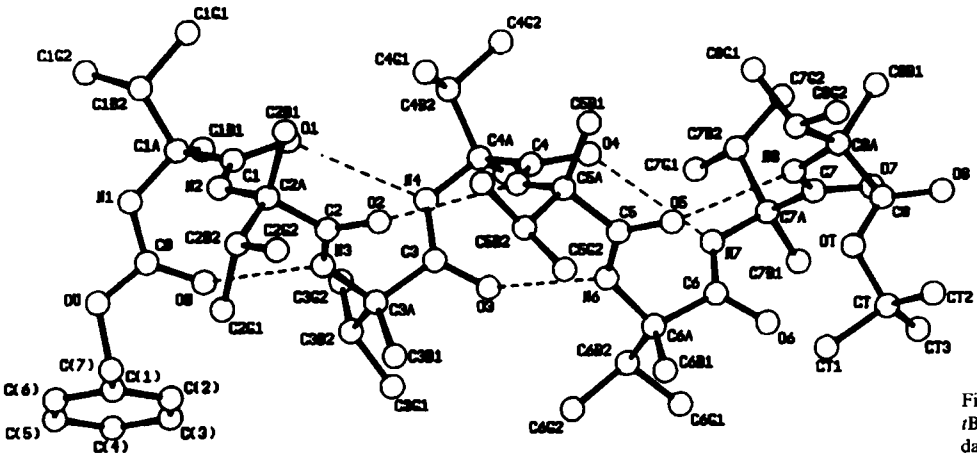

Fig. 4. Crystal structure of Z-[L-(αMe)Val]$_8$-O-*t*Bu. The intramolecular H-bonds are indicated by dashed lines.

Table 2. Selected torsion angles [°] for the homopeptides Z-[L-(αMe)Val]$_n$-O*t*Bu (n = 3, 6–8).

	Trimer	Hexamer Mol. A	Hexamer Mol. B	Heptamer	Octamer
θ^3	85.7(4)	60.8(4)	49.5(5)	57.0(5)	−79.8(6)
θ^2	132.5(3)	76.7(5)	86.8(6)	83.2(6)	−87.7(7)
θ^1	176.8(3)	177.2(3)	−177.1(5)	−170.3(5)	−178.5(5)
ω_0	−174.9(3)	−171.0(3)	−163.0(4)	−172.5(4)	−172.3(5)
ϕ_1	−59.5(4)	−61.3(5)	−63.0(5)	−59.2(5)	−56.8(7)
ψ_1	−26.1(3)	−33.9(5)	−29.8(5)	−32.5(5)	−32.6(6)
ω_1	−178.4(2)	−171.4(3)	−171.2(3)	−172.8(4)	−175.5(5)
ϕ_2	−59.0(3)	−56.0(5)	−53.0(5)	−55.2(5)	−51.9(7)
ψ_2	−24.8(3)	−25.9(5)	−30.2(5)	−25.1(5)	−25.1(7)
ω_2	180.0(2)	−172.8(3)	−172.4(4)	−177.7(3)	−173.5(5)
ϕ_3	−51.6(3)	−58.6(5)	−59.8(5)	−51.9(5)	−55.6(7)
ψ_3	−54.1(3) [a]	−24.1(5)	−19.9(5)	−27.9(6)	−23.8(7)
ω_3	175.9(2) [b]	−168.7(4)	−175.7(3)	−172.9(4)	−177.6(5)
ϕ_4	–	−54.8(5)	−57.9(4)	−57.9(6)	−50.7(7)
ψ_4	–	−28.1(5)	−23.5(5)	−17.9(6)	−30.7(7)
ω_4	–	−178.2(3)	−179.6(3)	−178.2(4)	−176.3(5)
ϕ_5	–	−57.2(4)	−56.3(4)	−54.9(5)	−50.6(8)
ψ_5	–	−43.7(4)	−39.2(4)	−24.1(5)	−35.1(8)
ω_5	–	−170.7(4)	−172.8(3)	−179.1(3)	−171.5(5)
ϕ_6	–	−57.0(6)	−52.6(4)	−60.2(5)	−49.0(8)
ψ_6	–	−54.3(5) [c]	−49.0(4) [e]	−27.8(6)	−39.4(8)
ω_6	–	175.0(4) [d]	174.5(3) [f]	−178.4(4)	−168.8(6)
ϕ_7	–	–	–	−46.4(5)	−62.2(8)
ψ_7	–	–	–	−49.5(5) [g]	−34.0(7)
ω_7	–	–	–	175.2(3) [h]	−174.3(5)
ϕ_8	–	–	–	–	−62.5(7)
ψ_8	–	–	–	–	3.0(10) [i]
ω_8	–	–	–	–	176.1(5) [j]
$\chi_1^{1,1}$	−73.4(3)	−64.4(4)	−70.6(5)	169.9(4)	169.6(6)
$\chi_1^{1,1'}$	160.6(3)	172.3(4)	165.1(5)	−66.1(4)	−66.6(6)
$\chi_2^{1,1}$	58.4(3)	63.2(5)	58.5(5)	54.5(7) [150.6(9)]	61.2(6)
$\chi_2^{1,1'}$	−67.1(3)	−171.0(4)	−174.4(4)	−155.8(6) [−62.0(11)]	−172.4(5)
$\chi_3^{1,1}$	166.4(3)	67.0(5)	63.6(6)	−167.9(5)	−163.6(5)
$\chi_3^{1,1'}$	−69.4(3)	−164.8(4)	−65.3(5)	68.1(5)	68.5(6)
$\chi_4^{1,1}$	–	63.3(5)	60.6(5)	−163.2(5)	64.7(7)
$\chi_4^{1,1'}$	–	−171.1(4)	−68.3(5)	70.2(5)	175.2(7)
$\chi_5^{1,1}$	–	169.6(4)	−68.6(4)	64.2(5)	−78.1(7)
$\chi_5^{1,1'}$	–	−64.7(4)	166.1(3)	−169.9(4)	151.3(9)
$\chi_6^{1,1}$	–	−68.1(5)	−70.2(3)	−69.1(5)	170.9(7)
$\chi_6^{1,1'}$	–	166.2(4)	164.5(3)	164.4(5)	−74.9(6)
$\chi_7^{1,1}$	–	–	–	−74.3(4)	−70.7(9)
$\chi_7^{1,1'}$	–	–	–	161.6(4)	146.5(10)
$\chi_8^{1,1}$	–	–	–	–	−69.1(6)
$\chi_8^{1,1'}$	–	–	–	–	166.7(5)

[a] N3-C3A-C3-OT. [b] C3A-CT-OT-CT. [c] N6-C6A-C6-OTA. [d] C6A-C6-OTA-CTA. [e] N16-C16A-C16-OTB. [f] C16A-C16-OTB-CTB. [g] N7-C7A-C7-OT. [h] C7A-C7-OT-CT. [i] N8-C8A-C8-OT. [j] C8A-C8-OT-CT.

Table 3. Intra- and intermolecular H-bond parameters for the homopeptides Z-[L-(αMe)Val]$_n$-O*t*Bu (n = 3, 6–8).

Peptide	Donor DH	Acceptor A	Symmetry operations of A	Distance/Å D···A	Distance/Å H···A	Angle/° D–H···A
Trimer	N3-H	Oø	x,y,z	3.118(3)	2.27(1)	168.4(1)
	N1-H	O2	$^1/_2+x,\,^1/_2-y,z$	3.054(3)	2.22(1)	164.8(1)
Hexamer	N3-H	OøA	x,y,z	3.313(5)	2.47(1)	167.0(1)
	N4-H	O1	x,y,z	3.217(4)	2.37(1)	167.5(1)
	N6-H	O3	x,y,z	3.056(4)	2.28(1)	150.4(1)
	N13-H	OøB	x,y,z	3.346(5)	2.49(1)	173.1(1)
	N14-H	O11	x,y,z	3.136(4)	2.28(1)	174.9(1)
	N15-H	O12	x,y,z	3.228(5)	2.37(1)	174.0(1)
	N16-H	O13	x,y,z	3.040(4)	2.24(1)	154.8(1)
	N11-H	O5	x,y,z	3.160(4)	2.32(1)	166.2(1)
	N1-H	O16	$1+x,y,1+z$	2.889(4)	2.06(1)	161.7(1)
Heptamer	N3-H	Oø	x,y,z	3.215(5)	2.37(1)	167.5(1)
	N4-H	O1	x,y,z	3.125(4)	2.27(1)	172.6(1)
	N5-H	O2	x,y,z	3.165(5)	2.32(1)	170.0(1)
	N6-H	O3	x,y,z	3.287(4)	2.43(1)	175.7(1)
	N7-H	O4	x,y,z	3.001(5)	2.16(1)	167.2(1)
	N1-H	O7	$x,y,z-1$	2.971(5)	2.20(1)	148.5(1)
Octamer	N3-H	Oø	x,y,z	3.041(6)	2.19(1)	169.7(1)
	N4-H	O1	x,y,z	3.194(5)	2.34(1)	176.6(2)
	N5-H	O2	x,y,z	3.149(5)	2.29(1)	173.6(1)
	N6-H	O3	x,y,z	3.075(5)	2.23(1)	167.1(1)
	N7-H	O4	x,y,z	3.244(5)	2.41(1)	164.2(1)
	N8-H	O5	x,y,z	3.086(6)	2.30(1)	151.9(1)
	N1-H	O7	$x,y,z-1$	2.960(5)	2.11(1)	169.2(2)

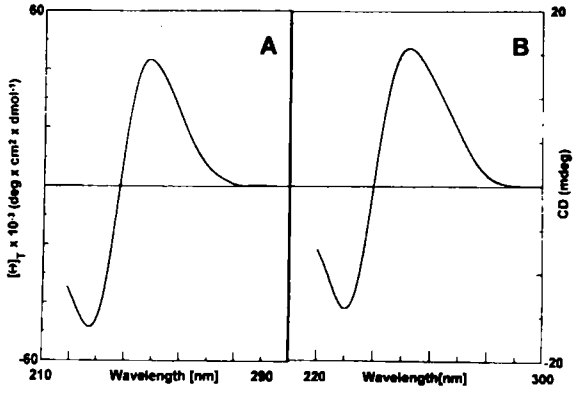

Fig. 5. CD spectra of *p*BrBz-[L-(αMe)Val]$_8$-O*t*Bu: **A**) in TFE solution (conc. 1 mM), where in the ordinate the *total* molar ellipticity is given, and **B**) in the solid state.

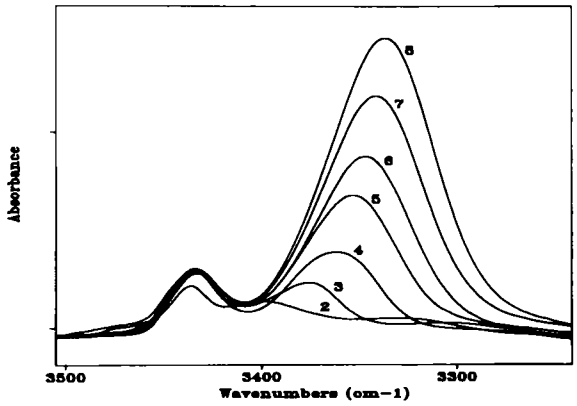

Fig. 6. FT-IR absorption spectra (3500–3250 cm^{-1} region) of the Z-[L-(αMe)Val]$_n$-O*t*Bu (n = 2–8) homopeptides in $CDCl_3$ solution (conc. 0.1 mM).

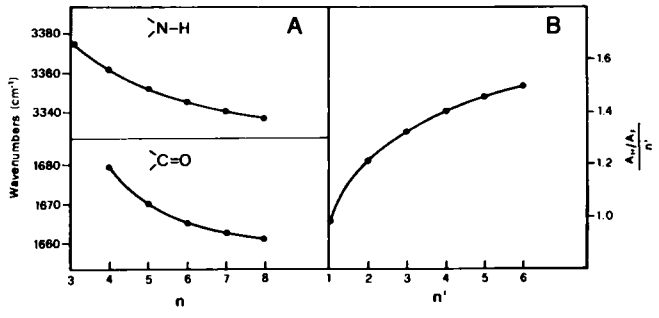

Fig. 7. A) Frequency variation of absorption maximum of the FT-IR absorption band of intramolecularly H-bonded N–H groups (upper part) and C=O groups (lower part) as a function of n, the number of residues in the homologous series Z-[L-(αMe)Val]$_n$-O*t*Bu (n = 3–8) in $CDCl_3$ solution (conc. 0.1 mM). B) Plot of the A_H/A_F over n' ratios as a function of n' (n' = 1–6, corresponding to n = 3–8), where n' is the number of intramolecular H-bonds of the 3_{10}-helices formed by the Z-[L-(αMe)Val]$_n$-O*t*Bu (n = 3–8) homopeptides in $CDCl_3$ solution (conc. 0.1 mM).

propan-2-ol) solutions by means of FT-IR absorption, ^{1}H NMR and CD techniques.

The most significant FT-IR results are illustrated in Figures 6 and 7. Several general conclusions can be drawn:

1) In $CDCl_3$ solution, where self-association is absent in the peptide concentration range examined (10–0.1 mM), as the peptide chain-length is enhanced, the frequencies of the absorption maxima of the stretching bands of intramolecularly H-bonded peptide N–H and C=O groups[7a, b] tend to decrease. This variation is steeper for the lower oligomers, whereas the curves tend to reach a plateau at about the octamer level. This finding suggests that in the isotactic [L-(αMe)Val]$_n$ series a fully developed intramolecularly H-bonded structure requires a minimum of eight residues.
2) In the plot of A_H/A_F over n' as a function of n' (where A_H/A_F is the ratio of the integrated intensities of the bands of H-bonded N–H groups to free N–H groups, and $n' = n - 2$ is the number of intramolecular H-bonds of the corresponding 3_{10}-helices) a trend parallel to the abscissa is expected when fully developed 3_{10}-helices are formed.[7a] Figure 7B shows that this is almost achieved for n' = 6 (octamer). The lower oligomers exhibit decreasing numbers of intramolecular H-bonds, but the values are still remarkably high for the penta-, hexa- and heptapeptides. Taken together, these results indicate that an intramolecularly H-bonded structure, most probably a 3_{10}-helix, is completely formed at the octamer level in $CDCl_3$ solution in the [L-(αMe)Val]$_n$ homopeptide series. The spectrum of the octamer in this halohydrocarbon is insensitive to heating at 25–55 °C.
3) In order to evaluate the relative contribution of the different components to the broad amide I absorption, centred at 1658 cm^{-1}, for the N–Ac octamer in TFE, a curve-fitting analysis was performed. The main component is a band at 1656 cm^{-1}, which is related to strongly intramolecularly H-bonded C=O groups[7a, b] and accounts for 68% of the total area. This value should be compared to 75%, the percentage of intramolecularly H-bonded C=O groups in the fully developed 3_{10}-helix of an N-acylated octapeptide ester. Interestingly, the spectral pattern for the hexamer is close to that of the octamer, whereas in the spectrum of the tetramer the bands related to free or weakly H-bonded carbonyls (1685–1670 cm^{-1} region)[7a, b] account for a much larger percentage than in the higher oligomers. The amide I and II regions in the spectrum of the octamer in DMSO are remarkably similar to those in TFE solution.

^{1}H NMR experiments were performed on the conformationally interesting Z-[L-(αMe)Val]$_8$-O*t*Bu, at 1 mM peptide concentration in $CDCl_3$, as a function of addition of the strong H-bonding acceptor solvent DMSO[20a–d] and the free radical TEMPO (2,2,6,6-tetramethyl-1-piperidyloxy)[20e] (Fig. 8).

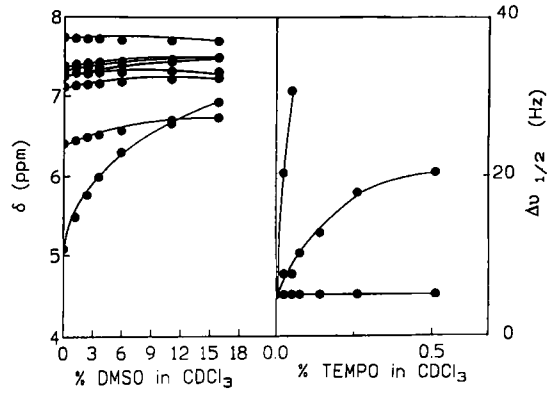

Fig. 8. Left: Plot of the NH chemical shifts in the ^{1}H NMR spectrum of Z-[L-(αMe)Val]$_8$-O*t*Bu as a function of increasing percentages of DMSO added to the $CDCl_3$ solution (*v*/*v*). Right: Plot of the bandwidth of the NH protons of the same peptide as a function of increasing percentages of TEMPO (*w*/*v*) added to the $CDCl_3$ solution. Peptide concentration 1 mM.

Among the various resonances of the NH protons we could assign unambiguously only that of the urethane N(1)H proton to the signal at highest field.[20c] On the basis of a comparison with a variety of model compounds[7a, 20c] we are also confident that the peptide N(2)H signal is next signal downfield of the N(1)H signal. The signals for the N(3)H through N(8)H protons are all found in the δ = 7.0–7.8 range. Their position in the spectrum, along with the insensitivity to the two perturbing agents, clearly show that the six NH signals N(3)H–N(8)H are intramolecularly H-bonded. It may be concluded that the secondary structure adopted in solution by the octamer is the 3_{10}-helix, in which the N(1)H and N(2)H protons are not expected to be involved in the intramolecular H-bonding scheme.[8] The helical structure of the octamer is stable to changing peptide concentration (in the 10–1 mM range) in $CDCl_3$ solution and to heating of the $CDCl_3$ solution to 55 °C and of the DMSO solution to 95 °C. The effect of temperature in the two solvents is illustrated in Figure 9. More specifically: 1) a very modest downfield shift (0.04 ppm) is only induced for the urethane NH proton by a 10-fold increase in peptide concentration in $CDCl_3$; 2) the absolute values for the temperature coefficients ($\Delta\delta/\Delta T$) in $CDCl_3$ are all lower than 2.8×10^{-3} ppm $°C^{-1}$;[20c] 3) a

0947-6539/96/0209-1108 $ 15.00+.25/0 Chem. Eur. J. 1996, 2, No. 9

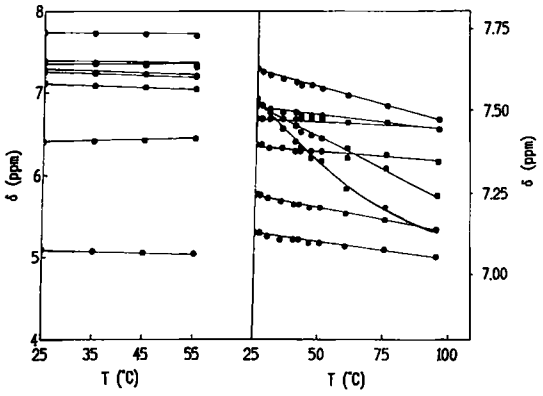

Fig. 9. Plots of the NH chemical shifts in the ^{1}H NMR spectrum of Z-[L-(αMe)Val]$_8$-O*t*Bu as a function of temperature in $CDCl_3$ (left) and in DMSO (right). Peptide concentration 1 mM.

more stringent test of helix stability, namely, the temperature dependencies of NH chemical shifts in DMSO solution,[20d] shows a bimodal distribution with two NH protons exhibiting significantly larger temperature coefficients (-5.7×10^{-3} and -3.8×10^{-3} ppm °C^{-1}) than all other NH protons (between -0.4×10^{-3} and -2.1×10^{-3} ppm °C^{-1}).

The CD spectra of three representative N$^{\alpha}$-acetylated [L-(αMe)Val]$_n$ oligomers (n = 4, 6, 8) in TFE in the region of absorption of the peptide chromophore are illustrated in Figure 10. It is evident that the spectral patterns above 200 nm of

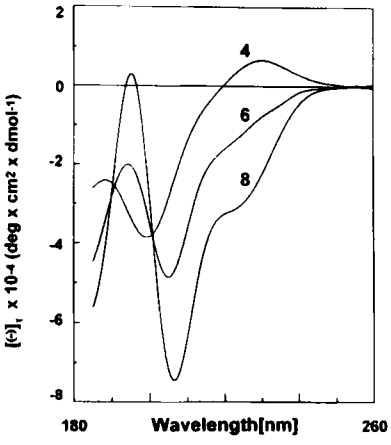

Fig. 10. CD spectra of the Ac-[L-(αMe)Val]$_n$-O*t*Bu (n = 4, 6, 8) homopeptides in TFE solution (conc. 1 mM). In the ordinate the *total* molar ellipticity is given.

the hexamer and octamer are similar. For both oligomers a negative Cotton effect near 207 nm is accompanied by a shoulder centred in the 222 nm region, with a ratio $R = [\theta]_{222}/[\theta]_{207}$ of about 0.3–0.4. In contrast, the spectrum of the tetramer differs significantly (the negative Cotton effect is below 200 nm, and the dichroism in the 220–250 nm region is positive). It is interesting to note that the complete far-UV CD spectrum of the octamer[21a] is qualitatively similar to the theoretically predicted spectrum for a right-handed 3_{10}-helix.[21b] In fact, in addition to the two optically active bands above 200 nm of different intensities, the ellipticity at about 195 nm is positive, although only slightly. The relatively low absolute ellipticity values are not surprising in view of the limited main-chain length of the peptide examined.[21b–d] The right-handed screw sense of the helical structure formed by the octamer in TFE is confirmed by the signs of the split CD curve of the N$^{\alpha}$-*para*-bromobenzoylated analogue (Fig. 5A).[19] Remarkably, heating the TFE solution to 55 °C or increasing the solvent polarity from TFE to HFIP does not cause any essential changes in the CD pattern of the octamer; the only variation is an approximately 20 and 15% decrease in the intensity of the 207 nm band and the 222 nm shoulder, respectively.

Conclusions

We have shown that in the crystal state as well as in solution the terminally blocked, isotactic homopeptides from the sterically constrained L-(αMe)Val residue form a type III β-turn at the trimer level, which evolves into a right-handed 3_{10}-helix in the longest oligomers (up to the octamer). This finding is in excellent agreement with the conclusions extracted from the conformational analysis of the homopeptide series from Aib, the achiral prototype of C$^{\alpha}$-tetrasubstituted α-amino acids.[7]

In the present X-ray diffraction study it was found that in the crystal state the end-to-end distance (from the carbonyl carbon of the N-blocking group to the carbonyl carbon of the C-terminal residue) is 6.1 Å for the L-(αMe)Val trimer, 12.1 Å for the regular 3_{10}-helix of molecule **B** of the hexamer, 14.4 Å for the heptamer and 16.1 Å for the octamer. The resulting average end-to-end distance per residue is in the 2.01–2.06 Å range. These data should be considered as particularly precise estimates, as they are obtained from high-resolution crystallographic investigations. However, it is remarkable that these homopeptides, although based on an extremely conformationally restricted residue, attain a stable, fully populated 3_{10}-helical structure only at approximately the octamer level. Nevertheless, the amount of 3_{10}-helix that is found in the oligomers from pentamer to heptamer is still significantly high.

Bearing in mind this limited flexibility, it is our contention that the [L-(αMe)Val]$_n$ series is undoubtely the best *chiral* homopeptide series investigated so far that can be exploited as a rigid molecular ruler in spectroscopic studies.

Experimental Section

Materials: The physical properties and the analytical data for the L-(αMe)Val homopeptides discussed in this work and their synthetic intermediates are listed in Table 1.

FT-IR Absorption: FT-IR absorption spectra were recorded with a Perkin-Elmer model 1720X spectrophotometer, flushed with nitrogen, equipped with a sample-shuttle device, at 2 cm^{-1} nominal resolution, averaging 100 scans. Solvent (baseline) spectra were recorded under the same conditions. Cells with path lengths of 0.1, 1.0 and 10 mm (with CaF_2 windows) were used. Spectrograde [D]chloroform (99.8% D) and DMSO were purchased from Merck, while TFE was obtained from ACROS.

^{1}H NMR spectra: ^{1}H NMR spectra were recorded with a Bruker model AM 400 spectrometer. Measurements were carried out in [D]chloroform (99.96% D; Merck) and in [D_6]DMSO (99.96% D_6; Fluka) with tetramethylsilane as the internal standard. The free radical TEMPO was purchased from Sigma.

Circular Dichroism: CD spectra were recorded immediately after peptide dissolution on a Jasco model J-715 spectropolarimeter. Cylindrical, fused quartz cells of 0.1 mm path lengths were employed. The data are expressed in term of $[\theta]_T$, the *total* molar ellipticity (deg cm^2 dmol^{-1}). 2,2,2-Trifluoroethanol (ACROS) and 1,1,1,3,3,3-hexafluoropropan-2-ol (Aldrich) were used as solvent.

X-Ray Diffraction: Data collection for the four peptides was performed on a Philips PW 1100 diffractometer. Crystallographic data are summarized in Table 4. The structures were solved by direct methods using the SHELXS 86 program [22a]. Refinements were carried out using the SHELXL 93 program [22b]. The thermal parameters were anisotropic for all non-H atoms of the trimer, hexamer, heptamer and octamer. All H-atoms for the four structures were allowed to ride on the

Table 4. Crystallographic data for the homopeptides Z-[L-(αMe)Val]$_n$-O*t*Bu (n = 3, 6–8).

	Trimer	Hexamer	Heptamer	Octamer
chem. formula	$C_{30}H_{49}N_3O_6$	$C_{48}H_{82}N_6O_9$	$C_{54}H_{93}N_7O_{10}$	$C_{60}H_{104}N_8O_{11}$
formula weight	547.7	887.2	1000.4	1113.5
cryst. solvent	ethyl acetate/petroleum ether	ethyl acetate/petroleum ether	methanol	methanol
cryst. size/mm	0.6 × 0.4 × 0.4	0.6 × 0.5 × 0.35	0.8 × 0.4 × 0.3	0.5 × 0.3 × 0.3
diffractometer	Philips PW1100	Philips PW1100	Philips PW1100	Philips PW1100
space group	$P2_12_12_1$	$P2_1$	$P2_1$	$P2_12_12_1$
cryst. system	orthorhombic	monoclinic	monoclinic	orthorhombic
a/Å	17.167(2)	25.412(2)	17.257(2)	18.631(2)
b/Å	19.410(2)	10.256(2)	9.677(2)	19.482(2)
c/Å	9.448(1)	20.888(2)	17.882(2)	18.518(2)
V/Å^3	3148.2(6)	5359.6(12)	2931.4(8)	6721.5(12)
α/°	90	90	90	90
β/°	90	100.1(1)	101.0(1)	90
γ/°	90	90	90	90
Z	4	4	2	4
T/K	293	293	293	293
$\lambda(Mo_{K\alpha})$/Å	0.7107	0.7107	0.7107	0.7107
ρ_{calcd}/g cm^{-1}	1.156	1.100	1.133	1.100
μ/cm^{-1}	0.80	0.76	0.78	0.76
scan mode	$\theta - 2\theta$	$\theta - 2\theta$	$\theta - 2\theta$	$\theta - 2\theta$
$2\theta_{max}$/°	56	56	56	56
measured refl.	4259	12168	7687	8822
unique refl.	4256	11833	7481	8816
refinement method	full matrix least-squares on F^2	full matrix-block least-squares on F^2	full matrix-block least-squares on F^2	full matrix-block least-squares on F^2
data/restraints/parameters	4255/0/352	11831/1/1111	7479/31/646	8815/6/700
goodness-of-fit (S), on F^2	0.887	0.805	0.893	0.715
$R(F)$/%, $I > 2\sigma(I)$ [a]	4.47	4.26	5.62	5.68
$wR(F^2)$/% (all data) [b]	14.15 [c]	13.12 [d]	17.69 [e]	18.72 [f]
resid. elect. density/e Å^{-3}	0.173/ − 0.217	0.168/ − 0.177	0.522/ − 0.266	0.365/ − 0.208

[a] $R = \sum||F_o| - |F_c||\sum|F_o|$. [b] $wR = [\sum w(F_o^2 - F_c^2)^2/\sum w(F_o^2)^2]^{1/2}$. [c] $w = 1/[\sigma^2(F_o^2) + (0.0908\,P)^2]$ with $P = (F_o^2 + 2F_c^2)/3$. [d] $1/[\sigma^2(F_o^2) + (0.0702\,P)^2]$ with $P = [\max(F_o^2, 0) + 2F_c^2]/3$. [e] $1/[\sigma^2(F_o^2) + (0.1013\,P)^2]$ with $P = (F_o^2 + 2F_c^2)/3$. [f] $1/[\sigma^2(F_o^2) + (0.0931\,P)^2]$ with $P = [\max(F_o^2, 0) + 2F_c^2]/3$.

attached atom during the refinement, with U set equal to 1.2 (or to 1.5 for methyl groups) the U_{eq} of the bound atom.

The E map corresponding to the best trial solution allowed the location of all 126 non-H atoms in the asymmetric unit of the hexamer (two independent molecules). The trial solution with the best combined figure of merit allowed the location of all non-H atoms of the heptamer, except the C^γ carbon atoms of the (αMe)Val[2] side chain. The C2G1 and C2G2 atoms of this residue, located on a successive ΔF map, were disordered over two sites. Their occupancy factors were refined to values of 0.58 and 0.42 for the major and minor components, respectively. The E map corresponding to the best trial solution allowed the location of 66 (out of 79) non-H atoms of the octamer. The remaining atoms were located on a successive ΔF map. Some disorder, as reflected by the high thermal parameters of the corresponding atoms, is observed for the Z-urethane phenyl ring atoms as well as for some C^γ atoms of the (αMe)Val residues at positions 4–7. Restraints were applied to the bond distances involving those atoms.

Crystallographic data (excluding structure factors) for the structures reported in this paper have been deposited with the Cambridge Crystallographic Data Centre as supplementary publication no. CCDC-1220-17. Copies of the data can be obtained free of charge on application to The Director, CCDC, 12 Union Road, Cambridge CB2 1EZ, UK (Fax: Int. code +(1223)336-033; e-mail: teched@chemcrys.cam.ac.uk).

Received: January 22, 1996 [F285]
Revised: April 1, 1996

[1] a) L. Stryer, R. P. Haugland, *Proc. Natl. Acad. Sci. USA* **1967**, *58*, 719–726; b) E. Haas, E. Katchalski-Katzir, I. Z. Steinberg, *Biopolymers* **1978**, *17*, 11–31; c) H. Tamiaki, K. Nomura, K. Maruyama, *Bull. Chem. Soc. Jpn.* **1994**, *67*, 1863–1871.

[2] a) S. S. Isied, A. Vassilian, *J. Am. Chem. Soc.* **1984**, *106*, 1732–1736; b) M. Y. Ogawa, I. Moreira, J. F. Wishart, S. S. Isied, *Chem. Phys.* **1993**, *176*, 589–600; c) M. Y. Ogawa, J. F. Wishart, Z. Young, J. R. Miller, S. S. Isied, *J. Phys. Chem.* **1993**, *97*, 11456–11463; d) M. Faraggi, M. H. Klapper, *J. Chim. Phys. Physicochim. Biol.* **1991**, *88*, 1009–1019; e) A. K. Mishra, R. Chandrasekar, M. Faraggi, M. H. Klapper, *J. Am. Chem. Soc.* **1994**, *116*, 1414–1422; f) T. Hayashi, T. Takimura, Y. Hitomi, T. Ohara, H. Ogoshi, *J. Chem. Soc. Chem. Commun.* **1995**, 545–546; g) G. Jones, II, L. N. Lu, V. Vullev, D. J. Gosztola, S. R. Greenfield, M. R. Wasiliewski, *Bioorg. Med. Chem. Lett.* **1995**, *5*, 2385–2390; h) N. Voyer, J. Lamothe, *Tetrahedron* **1995**, *51*, 9241–9284.

[3] a) B. Boulat, L. Emsley, N. Müller, G. Corradin, J. L. Maryanski, G. Bodenhausen, *Biochemistry* **1991**, *30*, 9429–9434; b) K. Wetz, H. Fasold, C. Meyer, *Anal. Biochem.* **1974**, *58*, 347–360; c) T. D. Yager, M. A. Reuben, P. R. Ainpour, E. Wickstrom, *FEBS Lett.* **1981**, *133*, 59–62; d) M. A. Reuben, P. R. Ainpour, H. L. Hester, V. L. Nevelin, E. Wickstrom, *Biochim. Biophys. Acta* **1981**, *654*, 11–25; e) A. Jain, S. G. Huang, G. M. Whitesides, *J. Am. Chem. Soc.* **1994**, *116*, 5057–5062.

[4] a) A. Yaron, F. Naider, *C. R. C. Crit. Rev. Biochem. Mol. Biol.* **1993**, *28*, 31–81; b) E. Benedetti, A. Bavoso, B. Di Blasio, V. Pavone, C. Pedone, C. Toniolo, G. M. Bonora, *Biopolymers* **1983**, *22*, 305–317; c) C. M. K. Nair, M. Vijayan, *J. Indian Inst. Sci.* **1981**, *63C*, 81–103.

[5] a) M. Goodman, C. Toniolo, P. Pallai in *Forum Peptides* (Eds.: B. Castro, J. Martinez), Dohr, Nancy, **1986**, pp. 146–174; b) C. Toniolo, G. M. Bonora, V. N. R. Pillai, M. Mutter, *Macromolecules* **1986**, *13*, 772–774.

[6] a) M. Goodman, A. S. Verdini, C. Toniolo, W. D. Phillips, F. A. Bovey, *Proc. Natl. Acad. Sci. USA* **1967**, *64*, 444–450; b) C. Toniolo, G. M. Bonora, *Makromol. Chem.* **1975**, *176*, 2547–2558; c) M. Goodman, C. Toniolo, F. Naider in *Peptides, Polypeptides and Proteins* (Eds.: E. R. Blout, F. A. Bovey, M. Goodman, N. Lotan), Wiley, New York, **1974**, pp. 308–319; d) C. Toniolo, G. M. Bonora, M. Mutter, *J. Am. Chem. Soc.* **1979**, *101*, 450–454.

[7] a) C. Toniolo, G. M. Bonora, V. Barone, A. Bavoso, E. Benedetti, B. Di Blasio, P. Grimaldi, F. Lelj, V. Pavone, C. Pedone, *Macromolecules* **1985**, *18*, 895–902; b) D. F. Kennedy, M. Crisma, C. Toniolo, D. Chapman, *Biochemistry* **1991**, *30*, 6541–6548; c) R. P. Hummel, C. Toniolo, G. Jung, *Angew. Chem. Int. Ed. Engl.* **1987**, *26*, 1150–1152; d) A. Bavoso, E. Benedetti, B. Di Blasio, V. Pavone, C. Pedone, C. Toniolo, G. M. Bonora, *Proc. Natl. Acad. Sci. USA*, **1986**, *83*, 1988–1992; e) V. Pavone, B. Di Blasio, A. Santini, E. Benedetti, C. Pedone, C. Toniolo, M. Crisma, *J. Mol. Biol.* **1990**, *214*, 633–635; f) C. Toniolo, E. Benedetti, *Macromolecules* **1991**, *24*, 4004–4009.

[8] C. Toniolo, E. Benedetti, *Trends Biochem. Sci.* **1991**, *16*, 350–353.

[9] C. M. Venkatachalam, *Biopolymers* **1968**, *6*, 1425–1436.

[10] a) C. Toniolo, M. Crisma, F. Formaggio, G. Valle, G. Cavicchioni, G. Précigoux, A. Aubry, J. Kamphuis, *Biopolymers* **1993**, *33*, 1061–1072; b) F. Formaggio, M. Pantano, G. Valle, M. Crisma, G. M. Bonora, S. Mammi, E. Peggion, C. Toniolo, W. H. J. Boesten, H. E. Schoemaker, J. Kamphuis, *Macromolecules* **1993**, *26*, 1848–1852; c) G. Valle, M. Crisma, C. Toniolo, S. Polinelli, W. H. J. Boesten, H. E. Schoemaker, E. M. Meijer, J. Kamphuis, *Int. J. Pept. Protein Res.* **1991**, *37*, 521–527; d) C. Toniolo, M. Crisma, G. M. Bonora, B. Klajc, F. Lelj, P. Grimaldi, A. Rosa, S. Polinelli, W. H. J. Boesten, E. M. Meijer, H. E. Schoemaker, J. Kamphuis, *ibid.* **1991**, *38*, 242–252.

[11] a) P. Wipf, R. W. Kunz, R. Prewo, H. Heimgartner, *Helv. Chim. Acta* **1988**, *71*, 268–273; b) P. Wipf, H. Heimgartner, *ibid.* **1988**, *71*, 258–267; c) D. Obrecht, U. Bodhal, C. Broger, D. Bur, C. Lehmann, R. Ruffieux, P. Schönholzer, C. Spiegler, K. Muller, *ibid.* **1995**, *78*, 563–580.

[12] W. H. Kruizinga, J. Bolster, R. M. Kellogg, J. Kamphuis, W. H. J. Boesten, E. M. Meijer, H. E. Schoemaker, *J. Org. Chem.* **1988**, *53*, 1826–1827.

[13] a) L. A. Carpino, E. S. M. E. Mansour, D. Sadat-Aalaee, *J. Org. Chem.* **1991**, *56*, 2611–2614; b) W. König, R. Geiger, *Chem. Ber.* **1970**, *103*, 788–798; c) L. A. Carpino, *J. Am. Chem. Soc.* **1993**, *115*, 4397–4398.

[14] IUPAC-IUB Commission on Biochemical Nomenclature, *Biochemistry* **1970**, *9*, 3471–3479.

[15] a) C. Ramakrishnan, N. Prasad, *Int. J. Protein Res.* **1971**, *3*, 209–231; b) R. Taylor, O. Kennard, W. Versichel, *Acta Crystallogr.* **1984**, *B40*, 280–288; c) C. H. Görbitz, *ibid.* **1989**, *B45*, 390–395.

[16] C. Toniolo, G. M. Bonora, A. Bavoso, E. Benedetti, B. Di Blasio, V. Pavone, C. Pedone, *Biopolymers* **1983**, *22*, 205–215.

[17] a) E. Benedetti in *Chemistry and Biochemistry of Amino Acids, Peptides and Proteins, Vol. 6* (Ed.: B. Weinstein), Dekker, New York, **1982**, pp. 105–184; b) T. Ashida, Y. Tsunogae, I. Tanaka, T. Yamane, *Acta Crystallogr.* **1987**, *B43*, 212–218.

[18] E. Benedetti, G. Morelli, G. Némethy, H. A. Scheraga, *Int. J. Pept. Protein Res.* **1983**, *22*, 1–15.

[19] a) C. Toniolo, F. Formaggio, M. Crisma, H. E. Schoemaker, J. Kamphuis, *Tetrahedron: Asymmetry* **1994**, *5*, 507–510; b) F. Formaggio, M. Crisma, C. Toniolo, J. Kamphuis, *Biopolymers* **1996**, *38*, 301–304.

[20] a) K. D. Kopple, M. Ohnishi, A. Go, *Biochemistry* **1969**, *8*, 4087–4095; b) T. P. Pitner, D. W. Urry, *J. Am. Chem. Soc.* **1972**, *94*, 1399–1400; c) G. M. Bonora, C. Mapelli, C. Toniolo, R. A. Wilkening, E. S. Stevens, *Int. J. Biol. Macromol.* **1984**, *6*, 179–188; d) J. D. Augspurger, V. A. Bindra, H. A. Scheraga, A. Kuki, *Biochemistry* **1995**, *34*, 2566–2576; e) K. D. Kopple, T. J. Schamper, *J. Am. Chem. Soc.* **1972**, *94*, 3644–3646.

[21] a) C. Toniolo, A. Polese, F. Formaggio, M. Crisma, J. Kamphuis, *J. Am. Chem. Soc.* **1996**, *118*, 2744–2745; b) M. Manning, R. W. Woody, *Biopolymers* **1991**, *31*, 569–586; c) T. S. Sudha, E. K. S. Vijakumar, P. Balaram, *Int. J. Pept. Protein Res.* **1983**, *22*, 464–468; d) E. K. S. Vijakumar, T. S. Sudha, P. Balaram, *Biopolymers* **1984**, *23*, 877–886.

[22] a) G. M. Sheldrick, *SHELXS 86. Program for the Solution of Crystal Structures*, University of Göttingen, Germany, 1986; b) G. M. Sheldrick, *SHELXL 93. Program for Crystal Structure Refinement*, University of Göttingen, Germany, 1993.